

Article

Coating of Ultra-Small Micro End Mills: Analysis of Performance and Suitability of Eight Different Hard-Coatings

Martin Bohley ^{1,*}, Ingo G. Reichenbach ¹, Sonja Kieren-Ehse ¹, Lukas Heberger ¹, Peter A. Arrabiyeh ¹, Rolf Merz ², Luisa Böhme ³, Julian Hering ⁴, Benjamin Kirsch ¹, Michael Kopnarski ², Eberhard Kerscher ³ , Georg von Freymann ^{4,5} and Jan C. Aurich ¹

¹ Institute for Manufacturing Technology and Production Systems, University of Kaiserslautern, Gottlieb-Daimler-Str., 67653 Kaiserslautern, Germany; ingogustav@gmail.com (I.G.R.); sonja.kieren-ehses@mv.uni-kl.de (S.K.-E.); lukas.heberger@mv.uni-kl.de (L.H.); peter.arrabiyeh@mv.uni-kl.de (P.A.A.); benjamin.kirsch@mv.uni-kl.de (B.K.); jan.aurich@mv.uni-kl.de (J.C.A.)

² Institute for Surface and Thin Film Analysis IFOS GmbH, Trippstadter Straße 120, 67663 Kaiserslautern, Germany; merz@ifos.uni-kl.de (R.M.); kopnarski@ifos.uni-kl.de (M.K.)

³ Working Group Materials Testing, University of Kaiserslautern, Gottlieb-Daimler-Str., 67663 Kaiserslautern, Germany; boehme@mv.uni-kl.de (L.B.); kerscher@mv.uni-kl.de (E.K.)

⁴ Department of Physics and Research Center OPTIMAS, University of Kaiserslautern, 67663 Kaiserslautern, Germany; hering@physik.uni-kl.de (J.H.); georg.freyermann@physik.uni-kl.de (G.v.F.)

⁵ Fraunhofer Institute for Industrial Mathematics, 67663 Kaiserslautern, Germany

* Correspondence: martin.bohley@mv.uni-kl.de; Tel.: +49-631-205-3472

Received: 26 February 2018; Accepted: 22 March 2018; Published: 29 March 2018



Abstract: Due to the constant need for better functionalized surfaces or smaller, function integrated components, precise and efficient manufacturing processes have to be established. Micro milling with micro end mills is one of the most promising processes for this task as it combines a high geometric flexibility in a wide range of machinable materials with low set-up costs. A downside of this process is the wear of the micro end mills. Due to size effects and the relatively low cutting speed, the cutting edge is especially subjected to massive abrasive wear. One possibility to minimize this wear is coating of micro end mills. This research paper describes the performance of eight different hard coatings for micro end mills with a diameter <math><40\ \mu\text{m}</math> and discusses some properties for the best performing coating type. With this research, it is therefore possible to boost the possibilities of micro milling for the manufacture of next generation products.

Keywords: micro milling; micro end mill; tool coating

1. Introduction

Individualized and miniaturized products are getting more common, especially for medical devices or electronic consumer products. To manufacture those products, extremely flexible and economic production processes are necessary [1]. One of the most promising processes for this task is micro milling with micro end mills. It combines a high geometrical flexibility with the possibility to machine almost any workpiece material. Especially when it comes to prototypes or the manufacture of small batch numbers, it is more economic compared to other micro production processes due to its low set-up costs [2].

Nevertheless, wear of the micro end mill is one of the limiting factors. It reduces surface quality and promotes burr formation as well as tool breakage. This is the reason why wear of micro end mills

has to be reduced to make micro milling even more competitive. In conventional machining, 85% of the tools are coated to reduce wear [3]. These coatings enhance tool life through a higher hardness, a higher resistance against abrasive wear, and a higher chemical stability [4]. Those coatings are not deeply researched when it comes to micro milling with micro end mills (diameter < 100 μm). Some work was done by the authors [5] or Uhlmann et al. [6] on TiN (titanium nitride) and diamond coated micro tools. All came to the same conclusion. The coating increased the radius of the cutting edges which in turn leads to higher friction, lower cutting capabilities and consequently, higher wear. This is the reason why the coating has to be extremely thin or the micro end mill optimized for roughing operations with a high feed per tooth [5].

The reasons for the higher wear are the size effects due to relatively high cutting edge radii [7] e.g., the rounded cutting edge radius is limited by the size of the cemented carbide grains—currently about 0.2 μm —and the thickness of the coating. Thus, the chip thickness is low compared to the cutting edge radius. This results in a high amount of ploughing which was originally formulated by Albrecht [8]. Because the minimal cutting edge radius r_g is limited by the currently available tool material, different strategies have to be chosen to reduce wear on the micro end mill. One of those strategies is coating the micro end mills with layer thicknesses as low as possible. In this paper, different coatings were tested on micro tapered end mills with a diameter < 40 μm to provide an insight in micro milling suited coatings. Therefore, the adhesion of different coating layers on the micro end mills were analyzed and the characteristics of the best performing coating described. Because conventional methods to characterize coatings are not applicable with these micro end mills due to possible size effects on up-scaled tools, FIB-cuts, nano-indentation tests, and micro-milling experiments were conducted.

2. Materials and Methods

Wear of micro end mills is mainly confined to the cutting edges. This is the reason why a single cutting edge design is ideal for research on tool wear. Every material removal has to be conducted by this cutting edge and thus, the behavior can be studied in depth. The single edge design chosen for this research was derived from the micro end mill design in Figure 1.

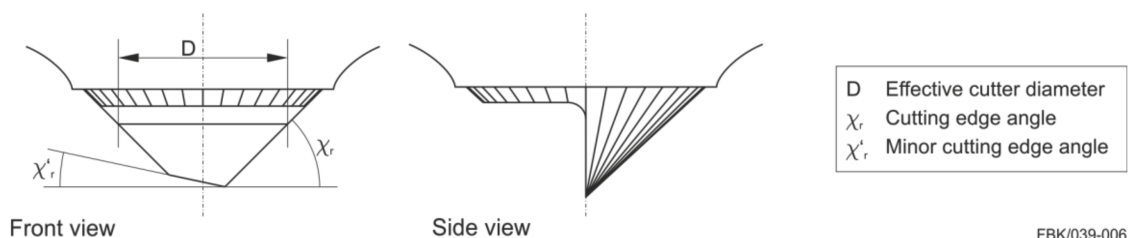


Figure 1. Geometry of a single edge micro end mill.

The micro end mill in this research had a minor cutting edge angle χ'_r of 12° and was optimized for a feed per tooth up to 3 μm . The cutting edge angle χ_r was 45° .

These micro end mills were made of cemented carbide with a grain size of 0.2 μm , 91% wolfram carbide, and 9% cobalt, a hardness of 1950 HV30 and a transverse rupture strength of 4700 N/mm². Its manufacture was conducted after [9] on a LT-Ultra MTC2501 (LT-Ultra Precision Technology GmbH, Aftholderberg, Germany) ultra-precision lathe. The ultra-precision lathe has a massive granite machine bed with hydrostatic axes in x - and z -directions. The straightness of the x -axis is 0.14 μm with a travel of 251 mm and straightness of the z -axis is 0.1 μm with a travel of 255 mm. The c -axis is an air bearing rotary axis with a maximum spindle speed of 2500 rpm, an axial spindle error of 0.051 μm and a run-out of 0.053 μm .

For tool manufacturing, a cemented carbide blank is mounted in the shrink fit chuck that guarantees a low run-out error on the c -axis of the machine tool (rotary axis). On the z -axis,

two hydrodynamic spindle motors hold the diamond grinding wheels (Figure 2). These motors have low vibrations and as a result, a low run-out of $<0.8 \mu\text{m}$ at a spindle speed of 12,500 rpm [10]. For the pre-grinding process, a resin bond grinding wheel with mesh #800 and a thickness of $250 \mu\text{m}$ was used. The grinding wheel for fine grinding was an electroplated bond with mesh #4800 and a thickness of $50 \mu\text{m}$. The process steps of the tool manufacturing are shown in Figure 3.

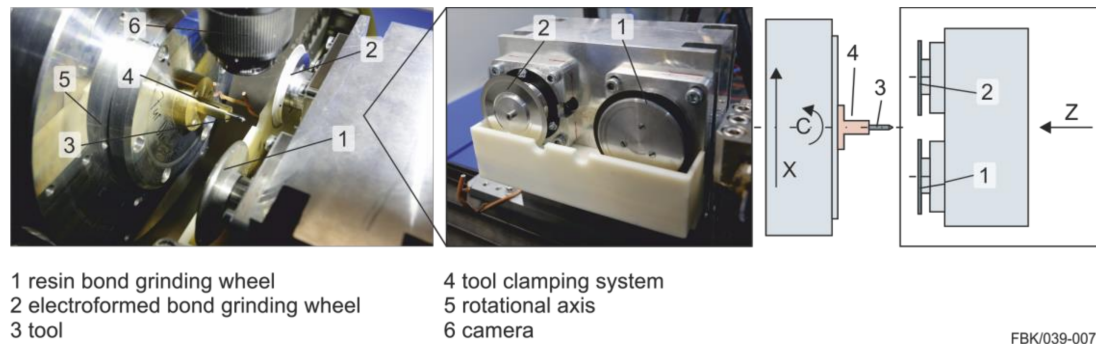


Figure 2. LT-Ultra MTC 250¹ rebuilt for micro end mill manufacture.

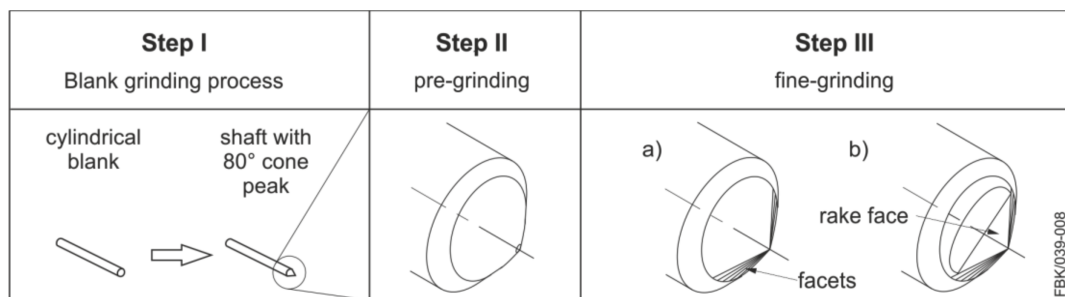


Figure 3. Process steps of tool manufacture. **Step I** blank grinding. **Step II** pre-grinding of a cone and **Step III** fine-grinding with (a) grinding of the facets (b) grinding the rake face.

Step 1 was conducted on a conventional tool grinding machine. The reason for this is the high amount of material to be removed to produce the cone on the tool blank. After this step, the blank with the cone tip was mounted in the shrink fit chuck on the ultra-precision lathe. Step 2 was performed with the resin bond grinding wheel to realize a comparably high material removal whereas Step 3 was performed with the fine grinding wheel to produce the desired geometry as accurately and smooth as possible. The facets shown in Step 3 were necessary because the ultra-precision lathe does not offer any free form generation (three-axis machine tool). Thus, the ideal geometry is approximated by linear movements resulting in these facets.

After grinding, the micro end mills were coated. Eight different coatings were examined: TiN, AlTiN, Al₂O₃, TiB₂, DLC (diamond like carbon), W-C:H, electroless plated diamond, and diamond (via CVD—chemical vapor deposition). The DLC coating as well as the diamond (CVD) were provided by an external supplier, all other were made in-house: TiN, AlTiN, W-C:H, and TiB₂ were produced in a physical vapor deposition (PVD) process with an Oerlikon Metco Domino Mini¹ system. Al₂O₃ was produced by a Picosun R-series atomic layer deposition reactor¹. The electroless plated diamond tools were produced with a system derived from [11].

TiN has a hardness of 2100 HV [12]. It is applied on the cemented carbide by means of a titanium interface layer. The interface layer increases adhesion. During the titanium coating, the addition of nitrogen is slowly increased, which results in a graded layer with its highest hardness on the surface. The coating thickness was $2.5 \mu\text{m}$.

The addition of aluminum to TiN results in an increased heat insulation of the tool; this protects the tool from damaging heat input which evolves in the contact zone due to friction and cutting [13]. This AlTiN coating is also harder than TiN with 3300 HV [14] and has already been successfully applied in previous works for micro milling applications [5]. The applied AlTiN had a thickness of 2.5 μm

Titanium based coatings form compounds with the oxygen in the environment on the surface and thus lead to the formation of titanium oxide (TiO_2) and, in the case of AlTiN, also to Al_2O_3 . Both TiO_2 and Al_2O_3 layers are softer than the Ti-based coating itself. This decomposition is a downside of Ti-coatings and leads to increased wear of the coating [15].

Al_2O_3 as a coating has a high resistance to oxidative wear due to the oxygen bound in the coating forming a stable composition [16]. Al_2O_3 is chemically inert and has a low thermal conductivity. The thermal conductivity property predestines Al_2O_3 as a coating for the thermal insulation of the tool [17]. With its hardness of 2300 HV [12], Al_2O_3 can additionally protect against abrasive wear. The Al_2O_3 coating thickness was 1 μm .

TiB_2 (titanium diboride) is a ceramic coating characterized by a high hardness of 4000 HV and chemical inertness [18]. The high hardness combined with a lower coefficient of friction (compared to TiN [18]) leads to the fact that this layer is highly wear-reducing. A challenge is the low adhesion to the substrate due to high residual compressive stresses in the coating [18]. However, as it is a titanium based coating, no additional adhesion layer has to be used, which makes it possible to produce hard and thin single layer coatings. The TiB_2 coating thickness was 0.2 μm , as determined as optimal thickness in [19].

Carbon-based coatings were also examined in this research, the so called diamond like carbon coatings (DLC), which W-C:H also belongs to. These layers are amorphous coatings with a predominant component of carbon and low hydrogen content. The amount of sp^2 -hybridized carbon leads to a low coefficient of sliding friction and at the same time a low hardness of the coating (1500 HV softer than the carbide substrate). This coating can act as a solid lubricant component. The reduction of friction in the contact zone can thus contribute to reducing abrasive wear [20]. DLC had a coating thickness of 3 μm and W-C:H had a thickness of 1.3 μm .

When it comes to diamond as a coating layer, diamond is a standard abrasive layer for grinding applications. This diamond is available in different sizes, which makes it also possible to be used in micro grinding applications. Here, the diameter of the diamond particles is much lower than 10 μm , down to the nanometer range, and the diamond is bonded to the cemented carbide by nickel with an electroless plating process [11]. This process can also be used to coat micro end mills. Due to the small particles, the cutting edge radius stays sharp and is protected against abrasive wear by the inert hardness of diamond. As it is the hardest material available, abrasive wear is low when machining non-iron materials. A downside of this electroless diamond coating is the nickel bond, which makes the layer softer. The electroless plated diamond thickness was 1.9 μm .

To increase the hardness, the cemented carbide was coated with diamond directly. This coating, applied via CVD (hereafter called Diamond CVD), has by far the highest hardness. At only slightly below 10,000 HV, it is almost as hard as natural diamond [21]. The nanocrystalline structure of the coating results in a low surface roughness, which means that less material adhesion is to be expected compared to uncoated tools [22]. The low surface roughness also ensures good chip flow and quickly dissipates the heat generated in the contact zone during machining [23]. Additionally, the coating is very resistant to abrasion. The diamond CVD-coating had a thickness of 2.4 μm .

After coating, test cuts were performed on an in-house developed three axes universal precision milling machine (UPMM). This machine tool is built up on a granite machine bed (Figure 4a,b). Air bearing linear axes are used in x - and y -direction with a travel of 140 mm. The z -direction is realized by a cross roller bearing axis with a travel of 60 mm. All axes are driven by stepper motors realizing an accuracy of <1 μm . On the z -axis, a palletizing system with a repeatability of about 2 μm is installed. With this system, it is possible to use this machine tool for machining when installing an air bearing spindle or as a measuring machine when installing a confocal microscope. This property

makes this machine tool universal for micro machining applications as the process result can be directly measured after machining.

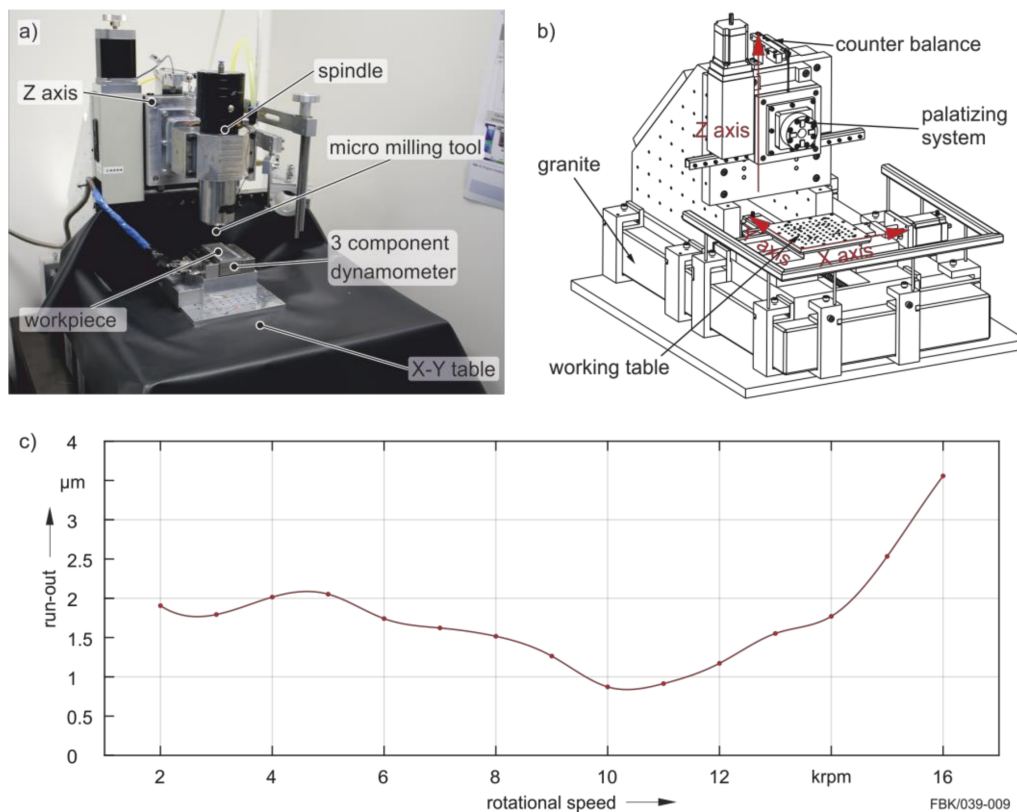


Figure 4. Universal precision machine tool. (a) overview, (b) isometric view and (c) run-out (peak-to-peak) of the air bearing spindle

For the test cuts, an ABL MM160¹ (Air Bearings Ltd, Ferndown, United Kingdom) air bearing spindle was used. This spindle can reach a spindle speed between 20,000 and 160,000 rpm with the characteristic shown in Figure 4c. The test cuts were performed at 90,000 rpm, thus the run-out at the tool tip was about 1.5 μm (peak-to-peak). The spindle speed was chosen, as it is an area with an average run-out error. This means that there is impact load on the micro end mill as well as the coating. When the micro end mill as well as the coating are able to withstand this, they are also capable of machining with a lower run-out error. On the other hand, if the run-out error is too high, tool breakage is very likely, thus preventing the evaluation of the coating's performance. All micro end mills were designed for a run-out of 3 μm which means there should be no unwanted contact between micro end mill and material to be cut (only the cutting edge penetrates the workpiece material). The feed per tooth was $f_z = 2 \mu\text{m}$ and the depth of cut $a_p = 25 \mu\text{m}$. This chip load in combination with the depth of cut is a proven parameter at our lab. It is a good compromise between surface quality, process stability, and tool wear. Lower feed rates result in higher ploughing and thus the tool wear increases. Higher feed rates result in higher stress levels of the tools which may result in tool breakage.

Each tool was tested in brass (CuZn40Pb2) with a travel path of only 200 mm to examine the initial wear. Brass was chosen as it is a common material in micro machining and often large areas need to be machined without tool change to keep the precision of the structure. Hence, tool wear is very crucial for machining these structures.

To reach the travel path of 200 mm, slots with a length of 25 mm were machined in brass with alternating feed direction. All machining tests were conducted without metal working fluids in a clean room environment with a temperature stability of $\pm 0.5 \text{ K}$.

3. Results

The test cuts showed three different types of wear of the coatings (Figure 5). The TiN and the W-C:H coatings provided adequate adhesion on the cemented carbide of the micro end mill. However, they were not hard enough to withstand the machining conditions, thus they showed abrasive wear at the cutting edge and on the rake face. This can be seen in FIB (focused ion beam) cuts for W-C:H in Figure 6. There, the thickness of the coating varies between 0.52 and 0.16 μm . The initial layer thickness was about 1.3 μm , thus there is not much coating left and the micro end mill wears out relatively fast. The DLC, Al_2O_3 , electroless plated diamond and the AlTiN coatings showed an almost immediate flake off. This means the adhesion on the micro end mill was not good enough although the layer itself should be sufficiently hard. In addition, when the Al_2O_3 ripped off, the geometry of the micro end mill was changed. The diamond (CVD) coating showed the same behavior. When the tool started to cut, the tip of the micro end mill broke off. This could be because the coating ripped off or because of the high coating temperatures of this process ($>900\text{ }^\circ\text{C}$) which may lead to a change in the material properties of the cemented carbide, causing premature failure.

The TiB_2 coating shows almost no wear after the test cut and no flake off. This means the coating is hard enough to withstand the machining conditions for a longer period of time. In another study, the most suitable layer thickness for this coating was determined [19]. The layer thickness exhibits two contradicting properties: the thicker the layer, the higher the residual stresses inside the layer (resulting in breakage of the coating); the thinner the layer, the lower the wear resistance. The ideal coating layer thickness for micro milling was determined to be 200 nm.

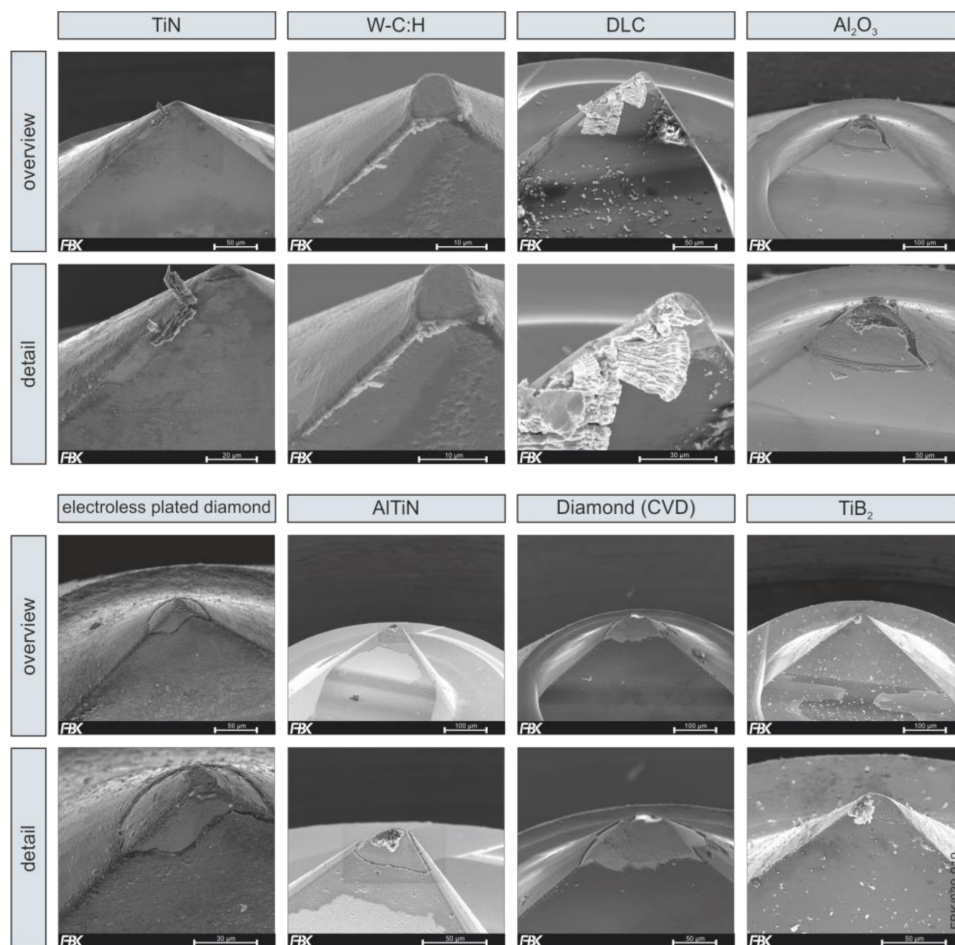


Figure 5. Coated micro end mills.

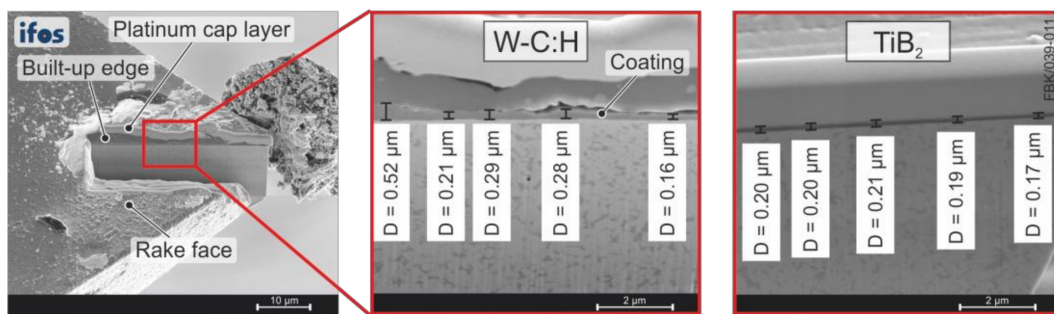


Figure 6. FIB cut at the tip of the micro end mill, coated with W-C:H (middle) and TiB₂ (right).

To examine the properties of the best performing layer (TiB₂) on the micro end mill, a FIB cut was done. Figure 6 shows the wear of a non-functioning W-C:H layer and the TiB₂ coating as a comparison.

Therefore, a cross section cut through the tip of the micro end mill was done by an ALURA 875 (FEI)¹ DualBeam focused ion beam (FIB). After deposition of a platinum cap layer on the surface to protect the original samples' topography and to avoid edge rounding, the cross section was cut by a 30 keV gallium ion beam. The cap layer can be seen in the SEM picture of Figure 6 as white layer, respectively as white bar in the detailed side view SEM picture.

For the W-C:H layer, below the cap layer in the side view of the cross section, an approximately 1 μm thick layer of brass (built-up edge) can be seen. Beneath, the W-C:H layer follows. It still forms a closed layer, but with an inhomogeneous layer thickness. The layer thickness was measured at five different positions of the cross section and varies over this distance from 0.16 μm up to 0.52 μm (unworn layer thickness ~1.3 μm). The existing cavities between the W-C:H layer and the adhered brass layer indicate local detachments of the brass layer. Beneath the W-C:H layer, the cemented carbide structure can be seen.

For the TiB₂, a homogeneous layer thickness can be seen. It varied only between 0.17 and 0.21 μm (unworn layer thickness ~0.2 μm). No built-up edge or defects are visible.

For further analysis of the best performing TiB₂ layer, instrumented indentation technique, also called depth sensing indentation, as introduced and described in detail by Oliver and Pharr [24,25] was performed. This technique has become widely used for the characterization of mechanical properties on the microscale. Hardness and other material parameters are derived from load and indentation depth data recorded continuously during the indentation procedure. The difficulty in characterizing coatings is associated with identifying the correct indentation load. On the one hand, it is recommended (in this case DIN EN ISO 14577-4 [26]) to use an indentation load that is small enough to avoid measurements being influenced by the substrate which would reduce the maximum hardness values. On the other hand, the roughness of the TiB₂ coating leads to a deviation of calculated and real contact area and will cause large scatter, especially when the indentation load is small. For these reasons, a polished cross section of the coated micro end mill cemented carbide tool shank was examined. The section was cut out, embedded, and polished with a diamond suspension (particle size down to 0.3 μm). The tests were then performed using the ASMEC Universal Nanomechanical Tester UNAT¹, equipped with a Synton¹ MDP diamond modified Berkovich indenter. In a first step, 156 positions for the indentation tests were set within a rectangular 380 × 35 μm measurement area including embedding, TiB₂ layer and substrate. The positions of the indentations were arranged in 20 rows, each with four indents with a distance of 10 μm to each other. The distance between adjacent columns is 10 μm and an additional 5 μm vertical offset was used to achieve a high resolution perpendicular to the surface of the milling tool as illustrated in Figure 7.

The testing procedure was as follows: In the loading segment, a linearly increasing loading rate was used to target a maximum value of 50 mN. After a 5 s dwell time, where load was kept constant, the indenter was unloaded again with a constant unloading rate. Then, the so called indentation hardness, which is the quotient of the maximum indentation load and the calculated value of the

projected contact area [27], was derived from the resulting load-indentation depth curve as described in detail in [28].

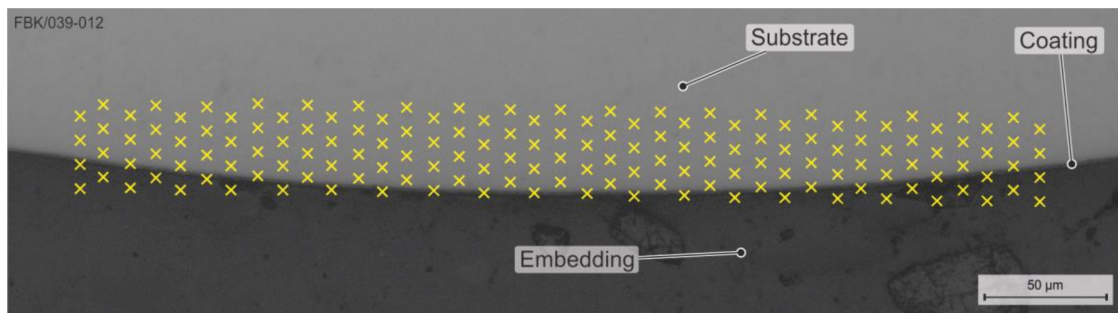


Figure 7. Microscopy image of the cross section of a TiB_2 coated cemented carbide tool shaft showing the measurement area and positions of indentation (×).

Figure 8a illustrates the dimensions of an indent in the substrate and its distance to neighboring indents. As can be taken from the figure, an indent has a diameter of about $1.8 \mu m$ and exhibits a minimum distance of $10 \mu m$ to its closest neighbors, as intended.

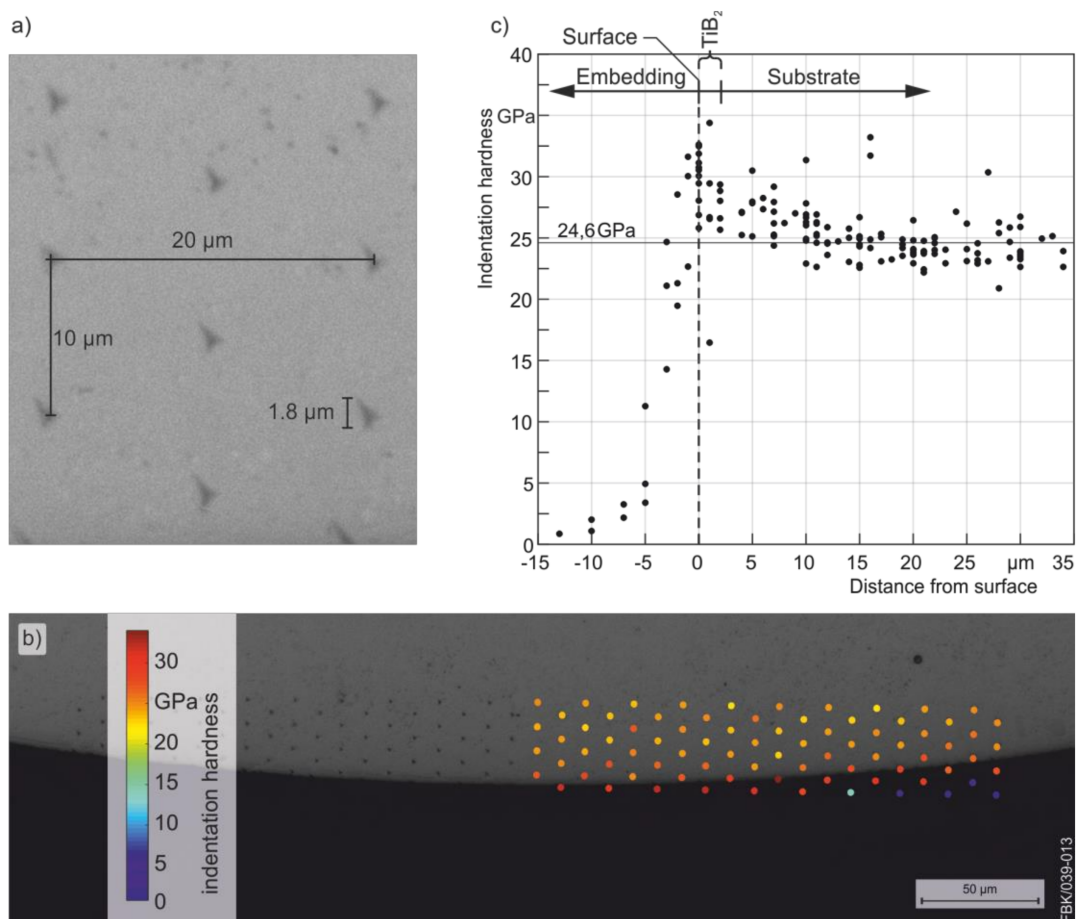


Figure 8. Results from instrumented indentation testing of a TiB_2 coated cemented carbide tool shaft: (a) geometry of an indent; (b) microscopy image showing the indents as well as indentation hardness; (c) indentation hardness plotted against the distance from the surface of the milling tool.

Figure 8b shows a light microscopy image of the cross section after indentation testing with the indents on the left, as well as superimposed colored dots on the right, with a color scale that indicates the indentation hardness obtained from experimental testing. As can be taken from the figure, hardness values scatter slightly in the substrate and considerably higher values were obtained in close proximity to the surface of the milling tool (i.e., in the TiB₂ layer), whereas the lowest values were obtained in the embedding.

In Figure 8c, the indentation hardness from all 156 measurements was plotted against the distance from the surface of the milling tool. The data points scatter around a course, which can be divided into three characteristic parts (embedding, TiB₂ layer, substrate). In the first part (embedding), the data points show a steep increase as getting closer to the surface of the milling tool. In the second part (TiB₂ layer), the hardness values reach a global maximum of about 34.4 GPa. Finally, in part three (substrate), the hardness values decrease and data points asymptotically approximate a mean value of about 24.6 GPa.

The indentation tests indicate that the hardness of the TiB₂ coating is in a range of 33 to 35 GPa, which is about 40% larger than the mean value of the substrate. Nevertheless, this value has to be looked at critically. Due to the small thickness of the coating, it is possible that measurements were influenced by the softer substrate or embedding and the exact value of the indentation hardness could be even higher. According to DIN EN ISO 14577-1 [28], the use of a modified Berkovich indenter allows for an approximation of the Vickers hardness (HV) by multiplying the calculated indentation hardness with a factor of 92.62. Thus, a value of about 3185 HV can be calculated from the maximum indentation hardness measured on the coating and a value of about 2278 HV can be calculated from the mean indentation hardness of the substrate. This means, the TiB₂ coating has a hardness of at least 3185 HV.

4. Conclusions

The coating of micro end mills with $D < 40 \mu\text{m}$ is a very promising technique to enhance wear resistance. So far, conventional coatings are not applicable for these small tools as they are too thick and reduce the cutting capabilities of the tool or they are not hard enough to withstand the high abrasive wear on the micro end mill's cutting edge. The only possibility to maintain the cutting capabilities in combination with a high wear resistance in the present study was the application of TiB₂ coatings. Due to the high hardness, the good surface adhesion, and the possibility to produce layers as small as 100 to 200 nm, it can enhance the quality of produced micro products or structures. The hardness of the coating is about 40% higher than that of the cemented carbide itself. This means the cutting capabilities should stay longer compared to uncoated tools. In further research, the possible increase in tool life of TiB₂ coated USM mills is going to be researched (also for commercially pure titanium) and compared to the tool life of uncoated micro end mills.

¹ "Naming of specific manufacturers is done solely for the sake of completeness and does not necessarily imply an endorsement of the named companies nor that the products are necessarily the best for the purpose."

Acknowledgments: This research was funded by the German Research Foundation (DFG) within the Collaborative Research Center 926 "Microscale Morphology of Component Surfaces". The authors also want to thank Jürgen Müller of Oerlikon Balzers Coating Germany GmbH for his competent and extraordinary help for adapting the coating system and the coatings to the micro end mills.

Author Contributions: Martin Bohley and Ingo G. Reichenbach conceived, designed, and performed the coating and micro milling experiments. Sonja Kieren-Ehse and Lukas Heberger supported in measurements and interpretation of the results. Rolf Merz and Michael Kopnarski performed the FiB cuts and the determination of the friction coefficients. Peter Arrabiyeh designed and performed the electroless plating experiments. Julian Hering and Georg von Freymann performed the Al₂O₃ coating. Lusia Böhme and Eberhard Kerscher designed, performed, and interpreted the indentation measurements. Benjamin Kirsch supervised the present study and helped to discuss and analyze the results. Jan C. Aurich initiated the study. All authors were highly involved in writing this paper.

Conflicts of Interest: The authors declare no conflict of interest.

References

1. Dornfeld, D.; Min, S.; Takeuchi, Y. Recent Advances in Mechanical Micromachining. *CIRP Ann. Manuf. Technol.* **2006**, *55*, 745–768. [[CrossRef](#)]
2. Thepsonthi, T. Modeling and Optimization of Micro-End Milling Process for Micro-Manufacturing. Ph.D. Thesis, Rutgers, The State University of New Jersey, Rutgers, NJ, USA, 2014.
3. Bobzin, K. High-performance coatings for cutting tools. *CIRP J. Manuf. Sci. Technol.* **2016**, *18*, 1–9. [[CrossRef](#)]
4. Prengel, H.G.; Pfouts, W.R.; Santhanam, A.T. State of the art in hard coatings for carbide cutting tools. *Surf. Coat. Technol.* **1998**, *102*, 183–190. [[CrossRef](#)]
5. Reichenbach, I.G.; Bohley, M.; Aurich, J.C. TiAlN coated ultra-small micro end mills. In Proceedings of the 15th International Conference of the European Society for Precision Engineering and Nanotechnology, Leuven, Belgium, 1–5 June 2015; pp. 321–322.
6. Uhlmann, E.; Oberschmidt, D.; Löwenstein, A.; Kuche, Y. Influence of Cutting Edge Preparation on the Performance of Micro Milling Tools. *Procedia CIRP* **2016**, *46*, 214–217. [[CrossRef](#)]
7. Xu, G. Einfluss der Schneidkantenform auf die Oberflächenausbildung beim Hochgeschwindigkeitsfräsen mit Feinkornhartmetall. Ph.D. Thesis, Technische Universität Darmstadt, Darmstadt, Germany, 1996.
8. Albrecht, P. New Developments in the Theory of the Metal-Cutting Process: Part, I. The Ploughing Process in Metal Cutting. *J. Eng. Ind.* **1960**, *82*, 348–357. [[CrossRef](#)]
9. Aurich, J.C.; Reichenbach, I.G.; Schueler, G.M. Manufacture and application of ultra-small micro end mills. *CIRP J. Manuf. Sci. Technol.* **2012**, *61*, 83–86. [[CrossRef](#)]
10. Bohley, M.; Reichenbach, I.G.; Müller, C.; Kirsch, B.; Aurich, J.C. Compact hydrodynamic spindle module for micromachining applications. In Proceedings of the 16th International Conference of the European Society for Precision Engineering and Nanotechnology, Nottingham, UK, 30 May–3 June 2016.
11. Arrabiyeh, P.A.; Kirsch, B.; Aurich, J.C. Development of Micro Pencil Grinding Tools via an Electroless Plating Process. *J. Micro Nano-Manuf.* **2017**, *5*, 11002. [[CrossRef](#)]
12. Ahmad, J. *Machining of Polymer Composites*; Springer: Boston MA, USA, 2009; ISBN 978-0-387-35539-9.
13. Tönshoff, H.K.; Denkena, B. Chip Formation. In *Basics of Cutting and Abrasive Processes*; Tönshoff, H.K., Denkena, B., Eds.; Springer: Berlin, Germany, 2013; ISBN 978-3-642-33256-2.
14. N.N. EXXTRAL—Die AlTiN-Basierte Schicht von Eifeler Für Die Hochleistungszerspanung. Available online: <http://www.eifeler.com/leistungen/pvd-schichtsysteme/exxtral-plus/> (accessed on 21 February 2018).
15. Wang, X.; Kwon, P.Y.; Sturtevant, C.; Kim, D.; Lantrip, J. Tool wear of coated drills in drilling CFRP. *J. Manuf. Process.* **2013**, *15*, 127–135. [[CrossRef](#)]
16. Schedler, W. *Hartmetall Für den Praktiker: Aufbau, Herstellung, Eigenschaften und Industrielle Anwendung Einer Modernen Werkstoffgruppe*; VDI-Verlag: Düsseldorf, Germany, 1988; ISBN 978-3540621195.
17. Klocke, F.; König, W. *Fertigungsverfahren 1: Drehen, Fräsen, Bohren*, 8th ed.; Springer: Berlin, Germany, 2007; ISBN 978-3-540-23458-6.
18. Berger, M.; Hogmark, S. Evaluation of TiB coatings in sliding contact against aluminium 2. *Surf. Coat. Technol.* **2002**, *149*, 14–20. [[CrossRef](#)]
19. Bohley, M.; Heberger, L.; Kirsch, B.; Aurich, J.C. Untersuchung des Verschleißverhaltens von TiB₂-beschichteten Mikrofräswerkzeugen. *ZWF Z. Wirtsch. Fabr.* **2017**, *112*, 598–601. [[CrossRef](#)]
20. N.N. Diamantähnliche Kohlenstoffschichten DLC (Diamond-Like Carbon). Available online: http://www.plascotec.de/downloads/DLC_Info.pdf (accessed on 11 January 2018).
21. Hintze, W.; Brüggemann, F.; Cordes, M. Entwicklung und Einsatzverhalten von Hartmetallwerkzeugen zum Bohren und Fräsen von Kohlenstoffverstärktem Kunststoff (CFK). In *Zerspanung Von und Mit Pulvermetallurgischen Werkstoffen*; Kolaska, H., Danninger, H., Biermann, D., Eds.; Heimdall Verlag: Rheine, Germany, 2017; ISBN 978-3-946537-32-8.
22. Henerichs, M.; Voß, R.; Harsch, D.; Kuster, F.; Wegener, K. Tool Life Time Extension with Nano-crystalline Diamond Coatings for Drilling Carbon-fibre Reinforced Plastics (CFRP). *Procedia CIRP* **2014**, *24*, 125–129. [[CrossRef](#)]
23. N.N. CCDia AeroSpeed CVD-Diamant. Available online: https://www.cemecon.de/sites/default/files/data_sheets/CemeCon_AeroSpeed_0.pdf (accessed on 21 February 2018).
24. Oliver, W.C.; Pharr, G.M. An improved technique for determining hardness and elastic modulus using load and displacement sensing indentation experiments. *J. Mater. Res.* **1992**, *7*, 1564–1583. [[CrossRef](#)]

25. Oliver, W.C.; Pharr, G.M. Measurement of hardness and elastic modulus by instrumented indentation: Advances in understanding and refinements to methodology. *J. Mater. Res.* **2004**, *19*, 3–20. [[CrossRef](#)]
26. DIN 14577-4. Available online: <https://www.beuth.de/en/standard/din-en-iso-14577-4/255107166> (accessed on 26 February 2018).
27. Meyer, E. Contribution to the Knowledge of Hardness and Hardness Testing. *Z. Ver. Deutsch. Ing.* **1908**, *52*, 740–835.
28. DIN 14577-1. Available online: <https://www.beuth.de/en/standard/din-en-iso-14577-1/190992638> (accessed on 26 February 2018).



© 2018 by the authors. Licensee MDPI, Basel, Switzerland. This article is an open access article distributed under the terms and conditions of the Creative Commons Attribution (CC BY) license (<http://creativecommons.org/licenses/by/4.0/>).